Co K-edge XAS study on a new cobalt-doped-SiO_2 pillared clay

Jin-Ho Choy,* Hyun Jung and Joo-Byoung Yoon

National Nanohybrid Materials Laboratory,
School of Chemistry and Molecular Engineering,
Seoul National University, Seoul 151-747, Korea.
Email:jhchoy@plaza.snu.ac.kr

New Co-doped-SiO_2-sol pillared montmorillonite has been synthesized by interlayer hydrolysis and condensation of tetraethylorthosilicate (TEOS) in the presence of Co^{2+} ion using an organic template. The Co K-edge XANES and EXAFS analyses for the CoO-SiO_2-PILC (before and after calcination) and for the references such as CoO and $Co(OH)_2$ were performed in order to obtain electronic and local structural information of cobalt species, which may act as a catalytic active site for the selective reduction of NO_x, hydrodesulfurization, and Fischer-Tropsch reaction. According to the XANES spectra, the divalent cobalt ion is stabilized in an octahedral symmetry. The EXAFS result shows a significant change in local symmetry around cobalt ion upon calcination. The EXAFS fitting result before calcination shows that the cobalt species is in the form of hydroxide, with a small number of (Co-Co) pairs compared to the bulk $Co(OH)_2$. After calcining at 550 ^oC, the first nearest neighbours were fitted to six oxygen atoms with two different distances, and the second and the third neighbours were fitted to two Si and one Co atoms. It is, therefore, reasonable to suggest a structure model, where the cobalt species on the SiO_2 sol exists as a nano cluster of $Co(OH)_2$ before calcination but transforms to a nanosized cobalt oxide covalently bound to the surface of SiO_2 pillar after calcination.

Keywords: pillared clay, porous material, de-NO_x reaction.

1. Introduction

In recent, a great effort has been made for the application of porous material as a selective reduction catalysts of nitrogen oxide compounds, so-called NO_x, which is a main atmospheric pollutant to cause acid rain, photochemical smog, and eventually ozone depletion (Fritz & Pitchon, 1997; Shelef, 1995). Conventionally, de-NO_x reaction has been achieved over various catalysts such as precious metals (Pt, Pt/Rh, Pd-Au, etc.; Iwamoto & Hamada, 1991), metal oxides ($SrFeO_3$, $CoAl_2O_4$, $YBa_2Cu_3O_7$, etc.; Meubus, 1977), and metal ion-exchanged zeolites (M^{n+}-ZSM-5, M^{n+} = Cu^{2+}, Co^{2+}, etc.; Iwamoto *et al.*, 1972). Pillared clays also can be regarded as promising de-NO_x catalyst because they have larger pore size than conventional zeolites, and moreover, pore dimension can be easily tuneable through proper selection of synthetic parameters (Choy *et al.*, 1998).

It is, therefore, necessary to characterize the catalytic active species in the substrate such as size, chemical phase, degree of dispersion, etc. In this regard, X-ray absorption spectroscopy is a powerful root to solve the electronic and geometric structures of achive species in the catalysts.

In the present study, therefore, our primary attention was not only paid to the preparation of a new de-NO_x catalyst by pillaring of mixed metal oxide sol particles in between silicate layers of clay, but also to probe the structure of active cobalt species in the de-NO_x catalyst using the X-ray absorption spectroscopy.

2. Experimental

New Co-doped SiO_2-sol pillared clay has been synthesized by an organic templating route (Galarneau *et al.*, 1995). The silicate layers of Na^+-montmorillonite were swelled in advance with hexadecyltrimethyl ammonium cation ($((CH_3)_4(CH_2)_{15}N^+:Q^+$), which was reacted subsequently with a mixed solution of tetraethylorthosilicate (TEOS), $CoC_{l2}\cdot 6H_2O$ and *n*-dodecyl amine ($C_{12}H_{25}NH_2$). The mixture was then reacted at room temperature for 24 h leading to the interlamellar hydrolysis and condensation of TEOS. Finally, organic templates were removed by calcining at 550 ^oC, in this way porous Co-doped SiO_2-sol pillared clays could be realized.

The Co K-edge X-ray absorption spectroscopy was carried out with synchrotron radiation using the extended X-ray absorption fine structure (EXAFS) spectroscopy facilities installed at the beam line 10B in the Photon Factory (KEK, Tsukuba), operated at 2.5 GeV with *ca.* 350 ~ 400 mA of stored current. The data were collected in transmission mode at room temperature. Absorbance was measured with the ionisation chamber filled with N_2 (25%) + Ar (75%) and N_2 (100%) for incident and transmitted beams, respectively. The data analyses for experimental spectra were performed by standard procedure as previously described (Konigsberger & Prins, 1988; Teo, 1986; Winick *et al.*, 1989). Photon energies of all the XANES spectra were calibrated by the first absorption peak of Co metal spectrum (E_0 = 7709 eV). The inherent background in the data was removed by fitting a polynomial to the pre-edge region and extrapolating it through the entire spectrum, from which it was subtracted. The absorbance $\mu(E)$ was normalized to an edge jump of unity for comparing the XANES features directly with one another. For EXAFS analysis using UWXAFS 2.0 code (Stern *et al.*, 1995), in the course of non-linear least-squares curve fitting between experimental EXAFS spectrum and theoretical one calculated by *ab-initio* FEFF6 code (Rehr et al., 1992), the structural parameters such as coordination number (N_i), bond distance (R_i), Debye-Waller factor (σ_i^2), and threshold energy difference (ΔE_0) were optimized as variables. The amplitude reduction factors of Co-O and Co-Co pairs were obtained from the reference compound of $Co(OH)_2$ and that of

Co-Si pair was fixed to 0.9, because no cobalt silicate reference compound was available.

3. Result & Discussion

Fig. 1 shows the Co K-edge XANES spectra for the CoO-SiO_2-PILC (before (d) and after (e) calcination) and for the references such as Co_3O_4 (a), CoO (b), and $Co(OH)_2$ (c). The pre-edge feature, originated from 1s $\rightarrow$ 3d transition, is observed at 7709 eV, which is a fingerprint for the site symmetry of cobalt species. The pre-edge and the edge onset positions of CoO-SiO_2-PILC are clearly different from those of Co_3O_4, but are the same as those of CoO and $Co(OH)_2$, representing that cobalt in the CoO-SiO_2-PILC is divalent. However, the pre-edge intensity of pillared clay was determined to be slightly lager than that of divalent cobalt references as shown in the inset of Fig. 1. Such a pre-edge due to 1s $\rightarrow$ 3d transition is in general dipolar-forbidden when the cobalt is stabilized in a centrosymmetric site, but quadruplely allowed with a low intensity. It is, therefore, reasonable to explain that some cobalt species of CoO-SiO_2-PILC is stabilized in a distorted octahedral symmetry or a coordinatively unsaturated site. It is worthy to note here that no change in the oxidation state and local symmetry of cobalt could be observed during the calcination process up to 550 ^oC.

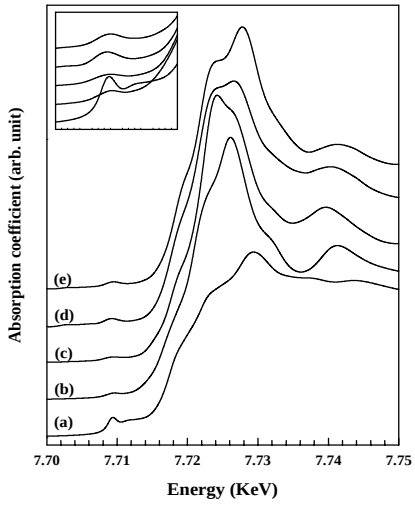

Figure 1
The Co K-edge XANES spectra for (a) Co_3O_4, (b) CoO, (c) $Co(OH)_2$, (d) before and (e) after the calcination of CoO-SiO_2-sol pillared clay. The inset shows the magnified pre-edge features.

The k^3-weighted EXAFS spectra and their Fourier transforms (FT) for the samples, before (c) and after (d) the calcination of CoO-SiO_2-sol pillared clay, CoO (a) and $Co(OH)_2$ (b) are shown in Fig. 2 (A) and (B), respectively. As shown in Fig. 2 (B), the first peak (1 – 2 Å) is ascribed to single scattering due to the first coordinated oxygens around central cobalt atom, and the next one (2 – 3.5 Å) is mainly from the second nearest neighbour such as Co atoms. The Fourier transforms feature of the sample before calcination, corresponding to (c) in Fig. 2 (B), is very similar with those (b) of $Co(OH)_2$ except the second peak intensity. And however, it changes dramatically after the calcination (d) as shown in Fig 2(B), where the second peak intensity was significantly reduced.

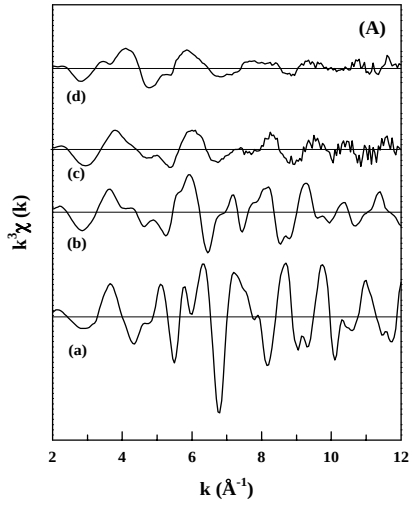

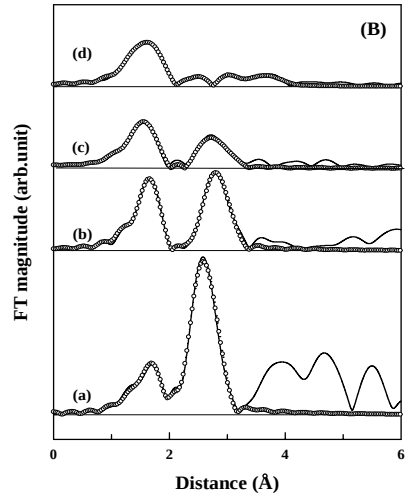

Figure 2
(A) The k^3–weighted EXAFS oscillation for (a) CoO, (b) $Co(OH)_2$, (c) before and (d) after the calcination of CoO-SiO_2-sol pillared clay
(B) The Fourier transforms (solid line) and fitting results (symbol) for (a) CoO, (b) $Co(OH)_2$, (c) before and (d) after the calcination of CoO-SiO_2-sol pillared clay .

In order to get more detailed structure of pillared clay, the Fourier-filtered EXAFS curve-fitting has been carried out and the structural parameters obtained are presented in Fig. 3 and Table 1, along with the results of reference materials of CoO (a) and $Co(OH)_2$ (b), those which are consistent with the previous literature one. It is found that the sample (c) shows only a small Co-Co coordination number (3.2) compared to the reference of

$Co(OH)_2$, indicating that the cobalt species exists as a very small cluster in the sample. Upon calcination, it is obvious that the cobalt species in pillared clay is significantly changed in its local structure, since even the first peak could not be fitted with single oxygen shell. However, two different oxygen shell fitting gives a more reasonable reliability factor. The R-space ranging from 2.1 to 4.5 Å was fitted with two different Si and one Co.

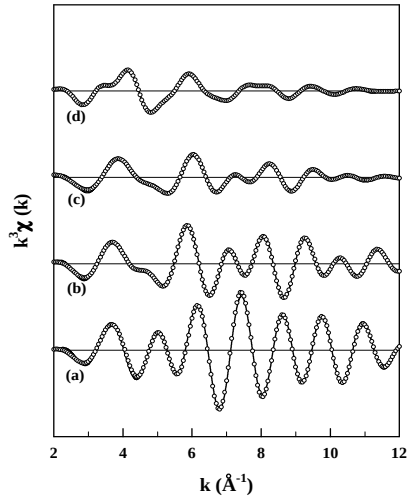

Figure 3
The EXAFS experimental (solid line) and fitting result (symbol) for (a) CoO, (b) $Co(OH)_2$, (c) before and (d) after the calcination of CoO-SiO_2-sol pillared clay.

On the basis of the above XANES and EXAFS results, it is possible to postulate a reliable structural model, where the cobalt species in the sample (c) before calcination exists as small clusters of $Co(OH)_2$, and however, these small hydroxide clusters transforms to cobalt oxide clusters and attaches on the surface of SiO_2 pillar. It is, therefore, concluded that the cobalt species are highly dispersed on the SiO_2 pillar surface in the CoO-SiO_2-PILC.

Table 1
The EXAFS fitting results for CoO (a), $Co(OH)_2$ (b), before (c) and after (d) the calcination of CoO-SiO_2-sol pillared clay.

Sample	Bond	Distance (Å)	N^a	σ^2 (10^{-3}Å^{-2})^b	E_0 shift(eV)
a	Co-O	2.13(1)	5.8(3)	7.6(2)	-0.5(5)
	Co-Co	3.00(0)	11.3(2)	8.1(1)	-0.9(3)
b	Co-O	2.09(0)	6	5.5(3)	-1.2(6)
	Co-Co	3.18(0)	6	7.8(4)	-1.2(2)
c	Co-O	2.04(1)	5.8(3)	9.7(7)	-2.3(14)
	Co-Co	3.13(4)	3.2(3)	9.9(9)	1.4(9)
d	Co-O_1	1.96(1)	1.9(2)	0.8(1)	-3.6(7)
	Co-O_2	2.12(1)	3.3(4)	1.7(2)	0.01(12)
	Co-Si_1	2.97(3)	2.3(6)	14.4(7)	-4.4(21)
	Co-Co	3.43(8)	1.1(3)	12.4(6)	-7.5(17)
	Co-Si_2	4.36(3)	9.6(2)	27.2(3)	3.0(15)

[a]. Coordination numbers
[b]. Debye-Waller factor

This work is financially supported by the Ministry of Education through Korea Research Foundation (1997-011-D0019) and BK 21 program, and by the Ministry of Science and Technology (NRL project).

Reference

Choy, J. H., Park, J. H. & Yoon, J. B. (1998). *J. Phys. Chem. B* **102**, 5991.
Fritz , A. & Pitchon, V. (1997). *Appl. Catal. B.* **13**, 1.
Galarneau, A., Barodawalla, A. & Pinnavaia, T. J. (1995) *Nature* **374**, 529.
Iwamoto, I., Maruyama, K., Yamazoe, N. & Seiyama, T. (1972). *J. Chem. Soc., Chem. Commun.* 615.
Iwamoto, M. & Hamada, H. (1991). *Catal. Today* **10**, 57.
Konigsberger, D. C. & Prins, R. *X-ray absorption. Principles, applications, techniques of EXAFS, SEXAFS and XANES*; Wiley: New York, 1988; pp. 444-457.
Meubus, P. (1977). *J. Electrochem. Soc.* **124**, 49.
Rehr, J. J., Zabinsky, S. I. & Albers, R. C. (1992). *Phys. Rev. Lett.* **69**, 3397.
Shelef, M. (1995). *Chem. Rev.* **95**, 209.
Stern, E. A., Newville, M., Ravel, B., Yacoby, Y. & Haskel, D. (1995). *Physica B* **208 & 209**, 117.
Teo, B. K. *EXAFS: Basic Principles and Data Analysis*; Springer-Verlag: Berlin, 1986; pp. 114-157.
Winick, H., Xian, D., Ye, M. & Huang, T. *Applications of synchrotron Radiation*, Gordon and Breach, 1989, p135-223

Received 31 July 2000 • Accepted 26 October 2000